

THERMAL DECOMPOSITION OF n-BUTANE AT HIGH TEMPERATURES

A Thesis Submitted
in Partial Fulfilment of the Requirements
for the Degree of
MASTER OF TECHNOLOGY

By
SUBBAIYAN SUBRAMANIAN

to the

DEPARTMENT OF CHEMICAL ENGINEERING
INDIAN INSTITUTE OF TECHNOLOGY KANPUR
JANUARY, 1981

CHE-1981-M-SUB-THE

I.I.T. KANPUR
CENTRAL LIBRARY

Acc. No. A 70640

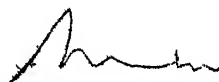
1 May 1982

665.773

su 162

CERTIFICATE

This is to certify that the work described in this thesis is the original work of Mr. Subbaiyan Subramanian performed under my supervision and has not been submitted elsewhere for a degree.



(S.V. Babu)

Professor

Department of Chemical Engineering
Indian Institute of Technology
Kanpur 208016, India

January 5, 1981

ACKNOWLEDGEMENT

I wish to express my sincere gratitude and indebtedness to my supervisor Professor S.V. Babu for his able guidance and active participation throughout the progress of this work.

My sincere thanks to Dr. M. Tyagaraju for his help and encouragement during the experimentation and computation work.

I express my appreciation and gratitude ^{to} Dr. R. Srivastava, Mr. K.M.S. Prasad and Mr. R.P. Yadav who helped me in some-way or other.

My thanks are due to Mr. M.M. Beg for his excellent typing and Mr. D.S. Panesar for his neat drawing.

S. Subramanian

S. SUBRAMANIAN

CONTENTS

	Page
LIST OF TABLES	v
LIST OF FIGURES	vi
CHAPTER	
I	INTRODUCTION 1
II	EXPERIMENTAL SETUP AND LASER SCATTERING SYSTEM 3
III	EXPERIMENTAL RESULTS 9
IV	KINETIC MECHANISM 10
V	NUMERICAL RESULTS AND DISCUSSION 16
	NOMENCLATURE 18
	REFERENCES 19
	APPENDIX 1 29
	APPENDIX 2 31

LIST OF TABLES

Table		Page
1	EQUILIBRIUM VALUES FOR FIVE SELECTED SHOCK SPEEDS	20
2	RANGES OF CONDITIONS FOR 9.8% $n\text{-C}_4\text{H}_{10}$ + Ar MIXTURE	20
3	ASSUMED MECHANISM AND RATE CONSTANT EXPRESSIONS USED IN COMPUTER SIMULATIONS	21

LIST OF FIGURES

Figure		Page
1	Schematic diagram of shock tube	22
2	Laser Schlieren signal and the corresponding calibration curve (i.e., photodiode output as laser beam sweeps across the knife edge) $P_1=1.68$ torr, $u_s=2.2492$ mm/ μ s, $T=2742$ K.	23
3 a.	Laser Schlieren signal in 9.8% $C_4H_{10} + Ar$ $P_1=4.32$ torr, $u_s=1.0304$ mm/ μ s, $T_2=1276$ K.	24
3 b.	Laser Schlieren signal in 9.8% $C_4H_{10} + Ar$ $P_1=3.92$ torr, $u_s=1.1353$ mm/ μ s, $T_2=1391$ K.	24
4 a.	Laser Schlieren signal in 9.8% $C_4H_{10} + Ar$ $P_1=6.08$ torr, $u_s=1.5965$ mm/ μ s, $T=1972$ K.	25
4 b.	Laser Schlieren signal in 9.8% $C_4H_{10} + Ar$ $P_1=7.80$ torr, $u_s=1.8779$ mm/ μ s, $T=2395$ K.	25
5	Concentration profiles for $T=1273$ K, $P_2/P_1=12.9$ and $C_4H_{10}:Ar=9.8:90.2$.	26
6	Concentration profiles for $T=1273$ K, P_2/P_1 $= 12.9$ and $C_4H_{10}:Ar = 9.8:90.2$.	27
7	Concentration profile for $P_2/P_1=16.5$, $T=1391$ K and $C_4H_{10}:Ar=9.8:90.2$.	28

ABSTRACT

THERMAL DECOMPOSITION OF N-BUTANE AT HIGH TEMPERATURES

Thermal decomposition of 9.8% n-butane + Argon was investigated in the temperature range 1060-3000K using shock tube - laser schlieren system. The density gradient profiles at different temperatures were got using the laser schlieren signals. An attempt was made to compare the experimental results with numerical results after assuming a detailed kinetic mechanism.

CHAPTER I

INTRODUCTION

Existing studies in the literature on the thermal decomposition of n-Butane can be divided into two groups according to temperature. Low temperature experiments ($T < 1000\text{K}$) are carried out in conventional reactors¹⁻⁴ using pure n-Butane. High temperature experiments ($T > 1000\text{K}$) are carried out in shock tubes⁵⁻⁷ with dilute n-Butane (mixture of n-Butane in an inert gas).

Thermal decomposition of hydrocarbons is carried out in shock tubes because of good reproducibility and the conditions can be varied over a wide range. Many investigations have been done on the thermal decomposition of hydrocarbons of low molecular weight (C_1 and C_2). The investigations on the thermal decomposition of n-Butane is incomplete. There are differences among the results at lower temperatures and the ones at higher temperatures. There is a marked difference in the data for the order of overall reaction, and there is a disagreement on the product distribution also. Some authors^{1,3} found the order of overall reaction to be 1 while Sagert and Laidler² and Blakemore, Barker, and Corcoran⁴ postulate the order to be $3/2$.

At higher temperatures there exist three studies. First one is by Wittig⁵, using a single pulse shock tube, the second one is by Izod, Kistiakowsky and Matsuda⁶, and the third one is by Fritz and Grönig⁷ using a shock tube coupled to a time-of-flight mass spectrometer.

In the present work, $n\text{-C}_4\text{H}_{10} + \text{Ar}$ mixtures containing 9.8% n-Butane were heated by incident shock waves over a temperature range 1060 - 3000K using shock tube laser-schlieren technique of Kiefer and Lutz⁸.

CHAPTER II

EXPERIMENTAL SETUP AND LASER SCHLIEREN SYSTEM

Experimental apparatus:

The experimental setup is completely described elsewhere⁹. A diagrammatic sketch of the experimental setup is shown in figure 1.

The shock tube:

The driver section consists of a 15.3 cm I.D. 1.68 m long stainless steel cylindrical tube. The low pressure section (i.e. the driven section or the test section) consists of a 9.85 cm I.D. 5.72 m long honed stainless steel cylindrical tube. The driver and driven sections are joined by an intermediate tapered stainless steel section which fits smoothly with the driver section on one side and with the driven section on the other side. This tapered section is permanently attached to the driver section. The driver and the driven sections can be locked together or unlocked by means of a coupling device. The entire assembly is mounted on wheeled iron stands which in turn are mounted on iron rails.

The driven section can be evacuated to a pressure of 2×10^{-5} torr using a 4" silicone oil pump backed by a roughing pump. The driver section is evacuated using a separate

mechanical pump. The combined leak and degassing rate in the driven section has been measured intermittently and found to be less than 5×10^{-5} torr. The pressure in the driver section is measured using a bourdon pressure gauge. The pressure in the driven section is measured using a silicone oil manometer. Shock waves are generated by bursting mylar sheets of thickness 0.005" by a pneumatically operated mechanical plunger which runs along the axis of the driver section. Mixtures of H_2, N_2 , He and CO_2 were used in the high pressure section to obtain the required variations in the shock velocities.

The shock speed was measured by means of gold resistance thermal gauges mounted flush with the walls of the shock tube. Since the shock wave attenuation was found to be negligible only two resistance gauges were used to obtain the shock velocity. The thin film gauges were prepared by vacuum deposition of gold on to glass tubes closed at one end. The $\frac{1}{2}$ " dia glass tubes were sealed at one end after inserting platinum wires. When this end was polished the cross section of platinum wires appear as small circles. Gold was then evaporated under vacuum on to this end to form a thin film of 1mm width making electrical contact between the two platinum leads.

The resistance of the thin film plate was continuously monitored during vacuum deposition and deposition was stopped

when the resistance reached 50 Ω . The thin films were mounted on the shock tube with the longer dimension perpendicular to the axis of the shock tube. The first gauge was placed at 4.25 m from the diaphragm and the second gauge was placed at 0.785 m from the first gauge. The windows for passing the laser beam were placed 5 cm after the second gauge. The resistance of the thin film gauges changes due to the passage of shock across them and it was converted to voltage signals which were suitably amplified and used to start and stop a Beckmann model 7370 digital counter. The time recorded by the digital counter was used to measure the shock speed. The rise time of the thin film gauges was found to be about 1 μ sec.

Gases:

High purity Matheson n-Butane (99.995%) and ultra high purity Argon (99.999%) from Indian Oxygen Ltd., were used.

Mixtures of n-Butane and Argon were prepared in a thoroughly evacuated stainless steel mixing chamber. The gasses are allowed to stand in the mixing chamber for 24 hours before use.

Laser Schlieren System:

The observation station i.e. the point where the laser beam passes through the shock tube was located 5 cm downstream of the

second film gauge and 3.5 cm before the end plate. The reflected shock wave did not interfere with the measurements because they (relaxation process) were usually completed within 10 μ sec. behind the incident shock whereas the reflected shock would arrive at the observation window only after 50-100 μ sec.

Glass windows of 1" dia in plexiglass adaptors were mounted flush with the wall of the shock tube. The windows were cleaned regularly with the lens paper to ensure gaussian distribution in the transmitted laser beam. The 6328 Å laser beam from a 0.5 mw Spectra Physics Model 156 He-Ne laser passed through the shock tube through these windows normal to the axis of the shock tube. Repeated runs in Argon, with the laser removed and realligned did not show any difference in the resolution, showing that the perpendicularity was good. The laser beam coming out of the shock tube was reflected by an aluminum mirror to fall on a knife edge. The distance from the shock tube centre to reflecting mirror was 1.35 m and the distance from the reflecting mirror to knife edge was 5.49 m. The part of the light that was not cut off by the knife edge was collected by a 7 cm dia lens and focussed to a H.P. type 5082-4203 pin-photodiode. The pin-photodiode along with the associated amplifier was mounted on a device which could be adjusted such that the photodiode receives all the light collected by the lens.

The knife edge could be moved smoothly to cut the laser beam. The pin-photodiode assembly, the glass lens and the knife edge were mounted on a smooth rigid bench. The laser and reflecting mirror were mounted on separate stands. The reflecting mirror was rotated at a slow uniform speed so that laser beam sweeps the knife edge at a uniform rate. The voltage output from the pin-photodiode as the beam sweeps across it is shown in figure 2. It is seen that the curve is linear in the centre and linearity extends to $\pm 20\%$ from the centre.

The photodiode output, suitably amplified, was fed through a Tek type 1A5 plug-in amplifier to a Tek type 549 storage oscilloscope. The oscilloscope was operated in a single sweep mode which was triggered by the signal from the thin film gauge just ahead of the observation station.

The overall response time of the system was measured by firing shocks into Argon. It was found that schlieren record decays with a time constant of 0.12μ sec. which may be taken as the time constant for the detection system. So schlieren records which showed time constants less than 0.35μ sec. were not used in analysis.

Procedure:

The driver and driven sections were locked together by means of a mylar diaphragm in between them. The driven section was evacuated to about 5 microns with the help of the two roughing pumps. The pressure was further brought down to about 5×10^{-5} torr using the diffusion pump. Runs taken with evacuation times varying from 2-10 hrs. did not show any difference and hence the evacuation was usually carried out for 2 hours. The driver section was evacuated using a roughing pump and was then filled with the gases of required composition and pressure. The knife edge was moved away from the lens and a chopper was placed in the path of the laser beam. This produced an a.c. signal from the pin-photodiode with its peak corresponding to full beam falling on the photodiode. Then the knife edge was brought back slowly cutting the light falling on the photodiode such that the peak voltage was equal to half the full beam voltage. The beam was thus centered and the chopper removed from the path of the beam. The test gas (i.e. mixture of n-Butane and Argon) was now filled into the driven section to the desired pressure and the shock was fired by releasing the mechanical plunger. The counter time was noted for shock speed calculations and the schlieren record stored in the oscilloscope was photographed.

CHAPTER III

EXPERIMENTAL RESULTS*

The shock speed was calculated by using the distance between the two film gauges and the counter time. The equilibrium values of the temperature, pressure, density etc were calculated for each shock speed by solving the mass, momentum and energy conservation relations by an iterative procedure on a computer. The mass, momentum and energy conservation relations are given in Gaydon¹⁴. A listing of the computer program used is given in Appendix 1. The specific heat data is taken from NASA SP 3001. The equilibrium values for five selected shock speeds are given in Table 1.

Density gradient profiles behind incident shock waves were obtained in 9.8% n-Butane + Argon mixture for five different temperatures in the temperature range 1060 - 3000K. The oscilloscope traces of the laser schlieren signals for the five different temperatures are shown in figures 2-4. Table 2 summarizes the range of experimental conditions for 9.8% butane + Argon mixture.

Density gradient profiles can be obtained numerically by solving the mass, momentum and energy relations, after assuming the detailed kinetic mechanism. The detailed kinetic mechanism is discussed in the next chapter.

CHAPTER IV

KINETIC MECHANISM

The pyrolysis of hydrocarbons are recognised as free radical chain reactions. Rice and Herzfeld¹⁰ first proposed the free radical mechanism in discussing these reactions. Sagert and Laidler², Wang, Rinker, and Corcoran⁴ and Purnell and Quinn¹¹ have proposed reaction schemes for the thermal decomposition of n-Butane, based on the Rice and Herzfeld type mechanism.

Initiation of chains in the pyrolysis of n-Butane is by the decomposition of n-Butane into two free radicals. Decomposition of n-Butane primarily takes place in chain propagation steps. The chain termination step of the mechanism is the bimolecular recombination of two free radicals.

Sagert and Laidler² have proposed an eight elementary step mechanism for the temperature range 793 - 863K. Wang et al³ have presented a 19 reaction mechanism for the temperature range 733 - 833K. They have considered the formation of propane, Butylene and the propagation of propyl radical. Blake more et al⁴ have investigated a 13 reaction mechanism in the temperature range 803 - 873K. They have encountered the

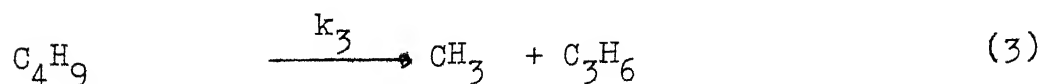
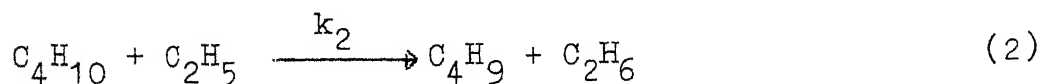
formation of Butylene and the propagation of propyl radical, but they have not considered the formation of propane. Very few investigations have been done at high temperatures. Fritz and Grönig⁷ have investigated the thermal decomposition of n-Butane in the temperature range 1170 - 1570K. They have coupled a shock tube to a time-of-flight mass spectrometer. They have developed a 21 reaction mechanism involving propane, Butene and propyl radical. Wittig⁵ has investigated the pyrolysis of n-Butane at 1400K using a single pulse shock tube. He has used a mechanism similar to that of Sagert and Laidler², Wang, Rinkerr and Corcoran³ and Prunell and Quinn¹¹ but modified for the conditions of high temperatures.

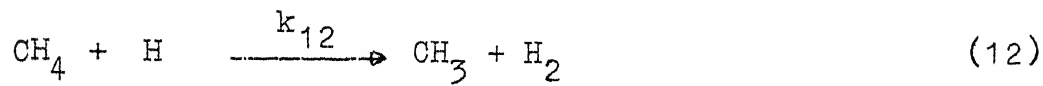
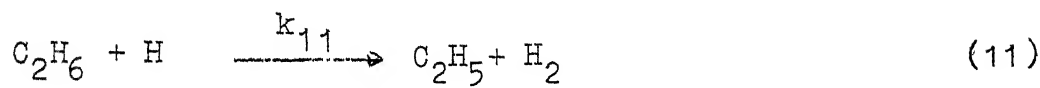
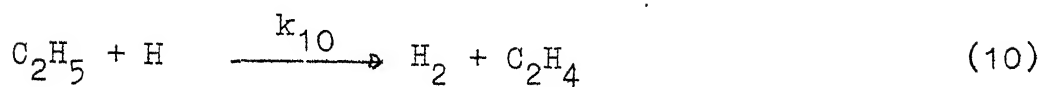
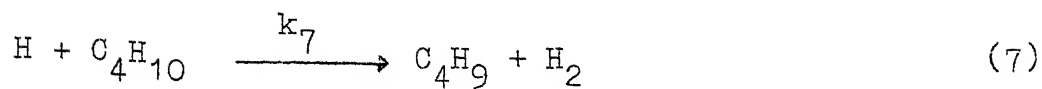
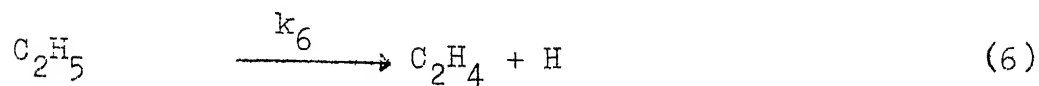
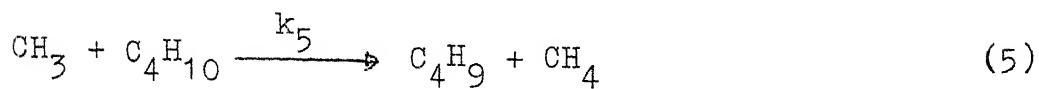
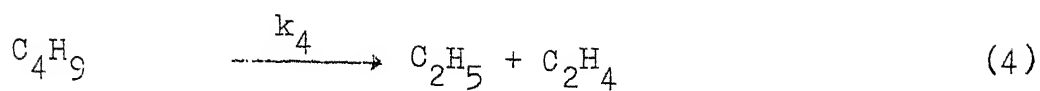
A free radical mechanism involving 14 elementary reactions is given below.

Chain Initiation:

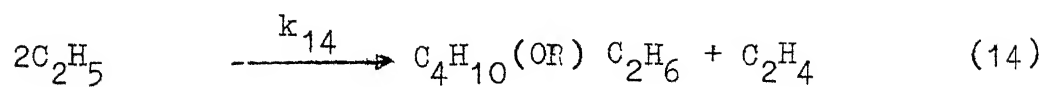


Chain Propagation:





Chain Termination:



In the mechanism given above the main products are ethylene, propylene, ethane and methane. Besides these main products there are reaction products such as hydrogen, traces of propane, traces of i-butane and components with higher carbon content. Acetylene and carbon were formed only at higher temperatures and longer reaction times. So they were not considered in the reaction mechanism.

The frequency factors, activation energies and the rate constants at 1273K for the above mechanism are given in Table 3.

In the mechanism given above there are 10 species. A mass balance is made for each component and the corresponding differential equations are given below. These equations are differential equations of concentration with respect to time.

$$\begin{aligned} \frac{d}{dt} [C_4H_{10}] = & -k_1 [C_4H_{10}] - k_2 [C_4H_{10}] [C_2H_5] - k_5 [C_4H_{10}] [CH_3] \\ & - k_7 [C_4H_{10}] [H] + k_{14} [C_4H_5]^2 \end{aligned} \quad (15)$$

$$\begin{aligned} \frac{d}{dt} [C_4H_9] = & k_2 [C_4H_{10}] [C_2H_5] - k_3 [C_4H_9] - k_4 [C_4H_9] \\ & + k_5 [C_4H_{10}] [CH_3] + k_7 [C_4H_{10}] [H] \end{aligned} \quad (16)$$

$$\frac{d [C_3H_6]}{dt} = k_3 [C_4H_9] \quad (17)$$

$$\begin{aligned} \frac{d [C_2H_6]}{dt} = & k_2 [C_4H_{10}] [C_2H_5] + k_8 [CH_3]^2 + k_9 [C_2H_5][H] \\ & - k_{11}[C_2H_6] [H] + k_{14} [C_2H_5]^2 \end{aligned} \quad (18)$$

$$\begin{aligned} \frac{d [C_2H_5]}{dt} = & 2k_1 [C_4H_{10}] - k_2 [C_4H_{10}] [C_2H_5] + k_4 [C_4H_9] \\ & - k_6 [C_2H_5] - k_9 [C_2H_5] [H] - k_{10} [C_2H_5][H] \\ & + k_{11}[C_2H_5][H] - k_{13} [C_2H_5][H] - 2 k_{14} [C_2H_5]^2 \end{aligned} \quad (19)$$

$$\begin{aligned} \frac{d [C_2H_4]}{dt} = & k_4 [C_4H_9] + k_6 [C_2H_5] + k_{10} [C_2H_5][H] \\ & + k_{14} [C_2H_5]^2 \end{aligned} \quad (20)$$

$$\frac{d [CH_4]}{dt} = k_5 [C_4H_{10}][CH_3] - k_{12} [CH_4][H] \quad (21)$$

$$\begin{aligned} \frac{d [CH_3]}{dt} = & k_3 [C_4H_9] - k_5 [C_4H_{10}][CH_3] - k_8 [CH_3]^2 \\ & + k_{12} [CH_4] [H] + 2 k_{13} [C_2H_5] [H] \end{aligned} \quad (22)$$

$$\begin{aligned} \frac{d [H_2]}{dt} = & k_7 [C_4H_{10}] [H] + k_{10} [C_2H_5] [H] + k_{11} [C_2H_6][H] \\ & + k_{12} [CH_4][H] \end{aligned} \quad (23)$$

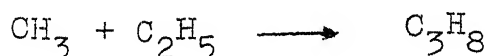
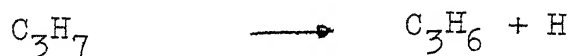
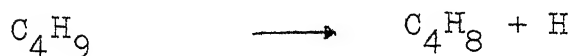
$$\begin{aligned} \frac{d[H]}{dt} = & k_6 [C_2H_5] - k_7 [C_4H_{10}][H] - k_9 [C_2H_5][H] - k_{10} [C_2H_5][H] \\ & - k_{11} [C_2H_6][H] - k_{12} [CH_4][H] - k_{13} [C_2H_5][H] \quad (24) \end{aligned}$$

The 10 first order differential equations (15) - (24) are solved simultaneously using numerical methods. The initial conditions for solving the above differential equations are initial concentration of the respective species. In this case all the initial concentrations except that of n-Butane are 0. After solving the above equations the concentration profiles of the different species can be drawn as shown in figures 5 - 7 .

CHAPTER V

NUMERICAL RESULTS AND DISCUSSION

A 19 reaction mechanism involving butylene, propane and propyl radical was also investigated. The reactions that were added to the earlier mentioned 14 reactions are as follows



The formation of butylene, propane and propyl radical was very small (of the order 10^{-20}) and it continued with longer times. So for the final computations the above five reactions have not been considered and the 14 reaction mechanism which has been discussed earlier is used.

The simultaneous differential equations are solved by the Hamming's predictor - corrector method. The algorithms

and computer program are described elsewhere¹². A listing of the program used is given in Appendix 2. The initial points for the Hamming's method are obtained by applying the Runge - Kutta method over the first three steps. Then the equations are solved over each step by applying the predictor and corrector algorithms alternately.

Figure 5 shows the concentration profiles for the decomposition of n-Butane and the formation of butyl, ethyl, methyl and hydrogen radical at 1273K. Figure 6 shows the concentration profiles for the formation of propylene, ethane, ethylene, methane and hydrogen at 1273K. Figure 7 shows the concentration for all the species at 1391K. Concentration computations were made till 2742K. At higher temperatures the decomposition of n-Butane is so fast that the integration step size for the time had to be given in the range 0.001 μ sec.

To make a comparison with the experimental results the differential equations involving the density and the temperature have to be coupled with the equations (15) - (24). The initial conditions for the density and the temperature are the equilibrium values (i.e. the frozen shock conditions). But unfortunately due to lack of time the last part could not be completed and is left for the future.

NOMENCLATURE

D_1	Initial density (g/cc)
D_2	Equilibrium density or density at frozen shock conditions (g/cc)
D_{21}	D_2/D_1
k_i	Rate constant (sec^{-1} or $\text{cm}^3 \text{ mole}^{-1} \text{ sec}^{-1}$), $i=1,14$
p_1	Initial pressure (torr or mm Hg)
p_2	Equilibrium pressure or pressure at frozen shock conditions (torr or mm Hg)
p_{21}	p_2/p_1
T_2, T	Temperature at frozen shock conditions or equilibrium temperature($^{\circ}\text{K}$)
u_s	Shock speed (mm/ μsec)
$[C_n H_m]$	Concentration of $C_n H_m$ (moles cm^{-3}) $n = 0,4$ and $m = 1,10$

REFERENCES

1. S. Sandler and Y. Chung, Ind. Eng. Chem. 53, 391 (1961).
2. N.H. Sagert and K.J. Laidler, Can.J. Chem. 41, 838 (1963).
3. Y.L. Wang, R.G. Rinker, A.W.H. Corcoran, Ind. Eng. Chem. Fund. 2, 161 (1963).
4. J.E. Blakemore, J.R. Barker, W.H. Corcoran, Ind. Eng. Chem. Fund. 12, 147 (1973).
5. S.L.K. Wittig, Phys. Fl. 12, Suppl. I-133 (1969).
6. T.P. Izod, G.R. Kistiakowsky, S. Matsuda, Journ. Chem. Phys. 56, 1337 (1972).
7. K. Fritz and E. Grönig, Proceedings of the 11th International Symposium on Shock Tubes and Waves, 383 (1977).
8. J.H. Kiefer and R.W. Lutz, Phys. Fl. 8, 1393 (1965).
9. V.V.N. Kishore, Ph.D. Thesis, I.I.T. Kanpur (1978).
V.V.N. Kishore, S.V. Babu and V. Subba Rao, Chem. Phys. 46, 297 (1980).
10. F.O. Pice and K.F. Herzfeld, J. Am. Chem. Soc. 56, 284 (1934).
11. J.H. Purnell and C.P. Quinn, Can.J. Chem. 43, 721 (1965).
12. B. Carnahan, H.A. Luther and J.O. Wilkes, Applied Numerical Methods (John Wiley and Sons, New York 1969).
13. D.B. Olson, T. Tanzawa and W.C. Gardiner, JR., Int. J. Chem. Kinetics, 11, 23 (1979).
14. A.G. Gaydon and I.R. Hurle, The Shock tube in High Temperature Chemical Physics (Reinhold Publishing Corporation, New York 1963).

TABLE 1

EQUILIBRIUM VALUES FOR FIVE SELECTED SHOCK SPEEDS

u_s mm/ μ sec.	T_2 K	p_1 mm Hg	p_2	D_{21}
1.027	1273.23	2.88	12.8521	3.0095
1.135	1341.33	3.92	16.5886	3.5548
1.596	1972.48	6.08	36.0070	5.4427
1.877	2395.23	7.80	50.9941	6.3474
2.091	2742.14	1.68	64.0433	6.9634

TABLE 2

RANGES OF CONDITIONS FOR 9.8% $n\text{-C}_4\text{H}_{10}$ + Ar MIXTURE.

p_1 mm Hg	u_s mm/ μ sec.	T_2 K
1.52 - 7.80	0.849 - 2.302	1060 - 3000

TABLE 3

ASSUMED MECHANISM AND RATE CONSTANT EXPRESSIONS USED IN
COMPUTER SIMULATIONS

Reaction	Frequency factor*	Activation energy Kcal mole ⁻¹	Rate constant at 1273K*	Reference
1	1.0×10^{17}	80.0	1.85×10^3	2
2	7.7×10^{11}	10.4	1.26×10^{10}	2
3	6.5×10^{11}	24.0	4.93×10^9	2
4	1.6×10^{10}	22.0	2.68×10^8	2
5	2.7×10^{11}	9.0	7.70×10^{11}	2
6	3.0×10^{14}	39.5	4.97×10^9	2
7	1.0×10^{14}	7.9	4.40×10^{13}	2
8	1.0×10^{11}	0.0	1.00×10^{11}	3
9	1.0×10^{13}	0.0	1.00×10^{13}	13
10	1.7×10^{12}	0.0	1.70×10^{12}	13
11	1.3×10^{14}	9.4	3.25×10^{12}	13
12	7.2×10^{14}	15.1	1.89×10^{12}	13
13	3.7×10^{13}	0.0	3.71×10^{13}	13
14	1.6×10^{13}	0.0	1.60×10^{13}	2

* In the units sec⁻¹ or cm³ mole⁻¹ sec⁻¹.

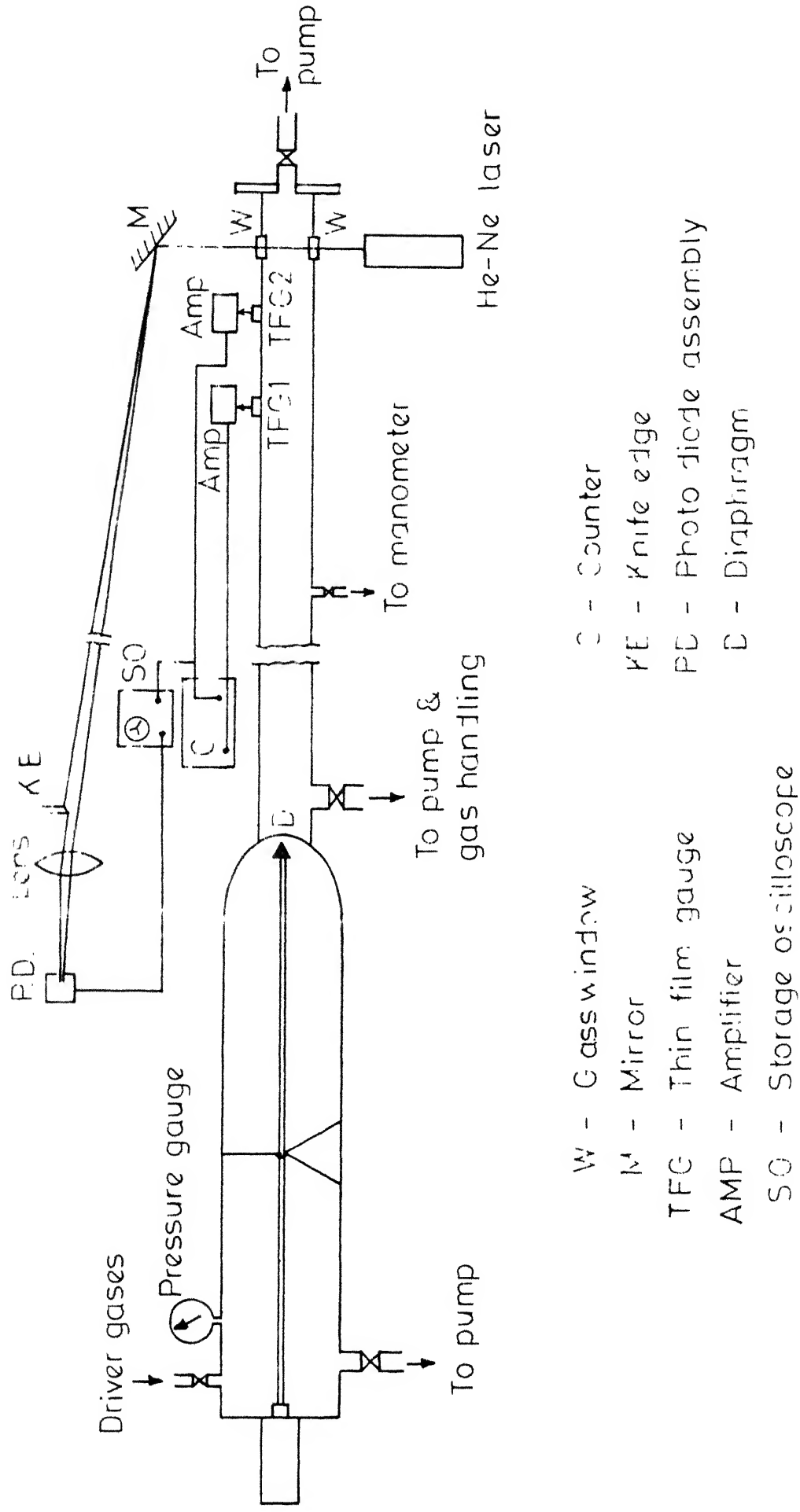


Fig. 1 - Schematic diagram of shock tube.

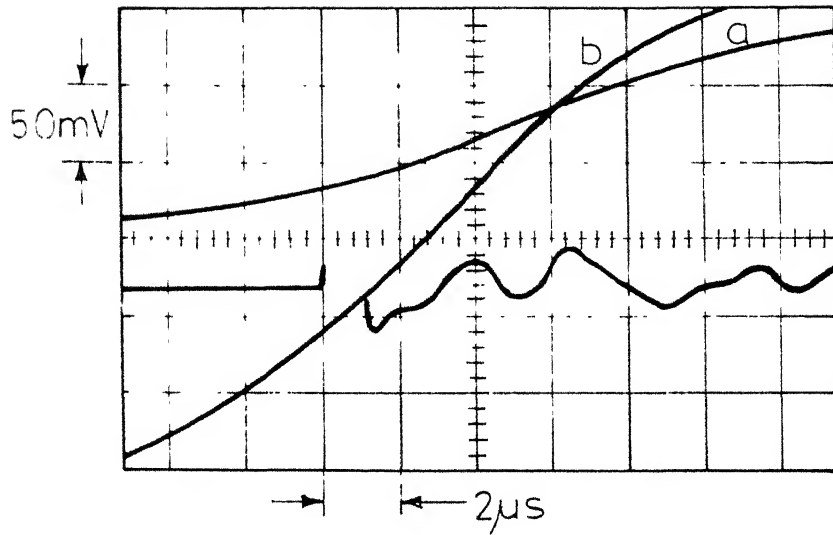


Fig 2 - Laser Schlieren signal and the corresponding calibration curve (i.e photodiode output as laser beam sweeps across the knife edge)

$p_1 = 1.68 \text{ torr}$, $u_s = 2.2492 \text{ mm}/\mu\text{s}$, $T = 274.2^\circ\text{K}$

Calibration trace: Horizontal scale = $0.5 \mu\text{s}/\text{div}$

Vertical scale

Curve a = $0.5 \text{ Volts}/\text{div}$.

Curve b = $0.2 \text{ Volts}/\text{div}$.

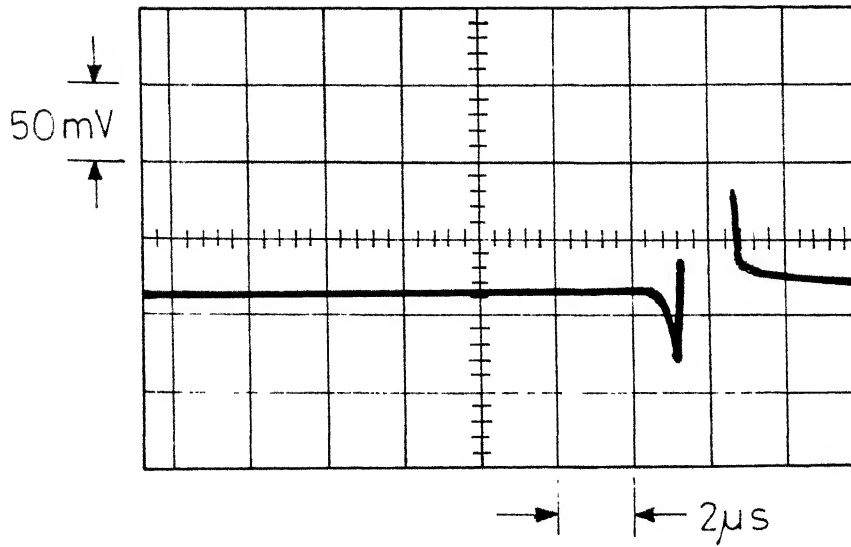


Fig. 3a - Laser Schlieren signal in 9.8% $C_4H_{10} + Ar$
 $p_1=4.32$ torr, $u_s=1.0304$ mm/ μ s, $T_2=1276$ °K

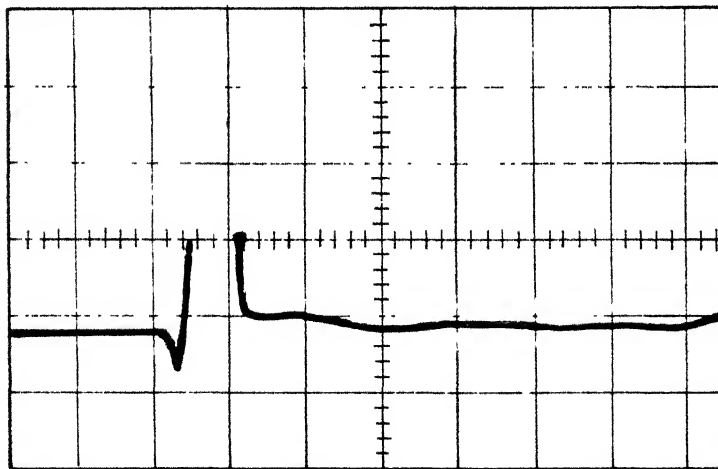


Fig. 3b - Laser Schlieren signal in 9.8% $C_4H_{10} + Ar$
 $p_1=3.92$ torr, $u_s=1.1353$ mm/ μ s, $T_2=1391$ °K.

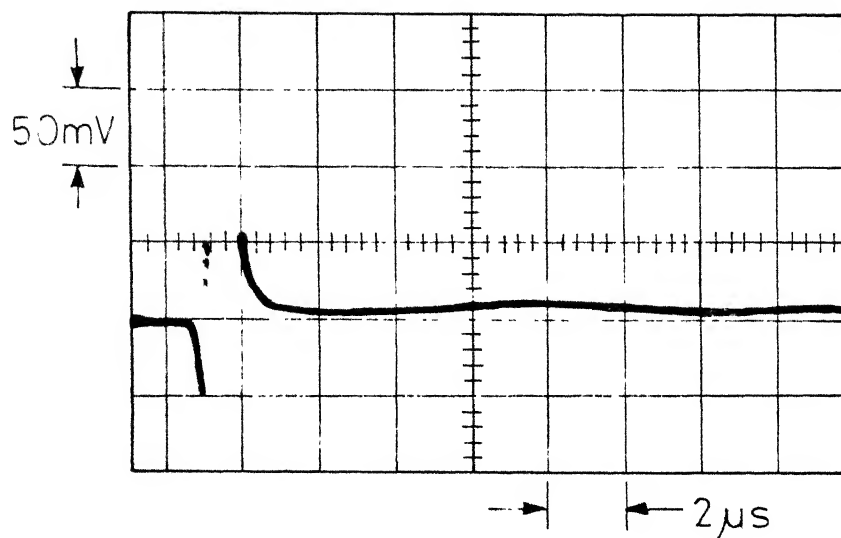


Fig. 4 a - Laser Schlieren signal in 9.8 % C_4H_{10} + Ar.
 $p_1=6.08$ torr , $u_s=1.5965$ mm/ μ s , $T=1972$ °K.

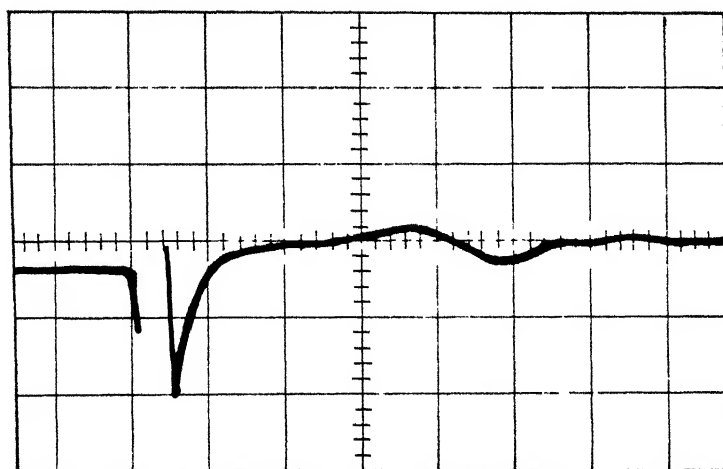


Fig. 4 b - Laser Schlieren signal in 9.8 % C_4H_{10} + Ar.
 $p_1=7.80$ torr , $u_s=1.8779$ mm/ μ s , $T=2395$ °K.

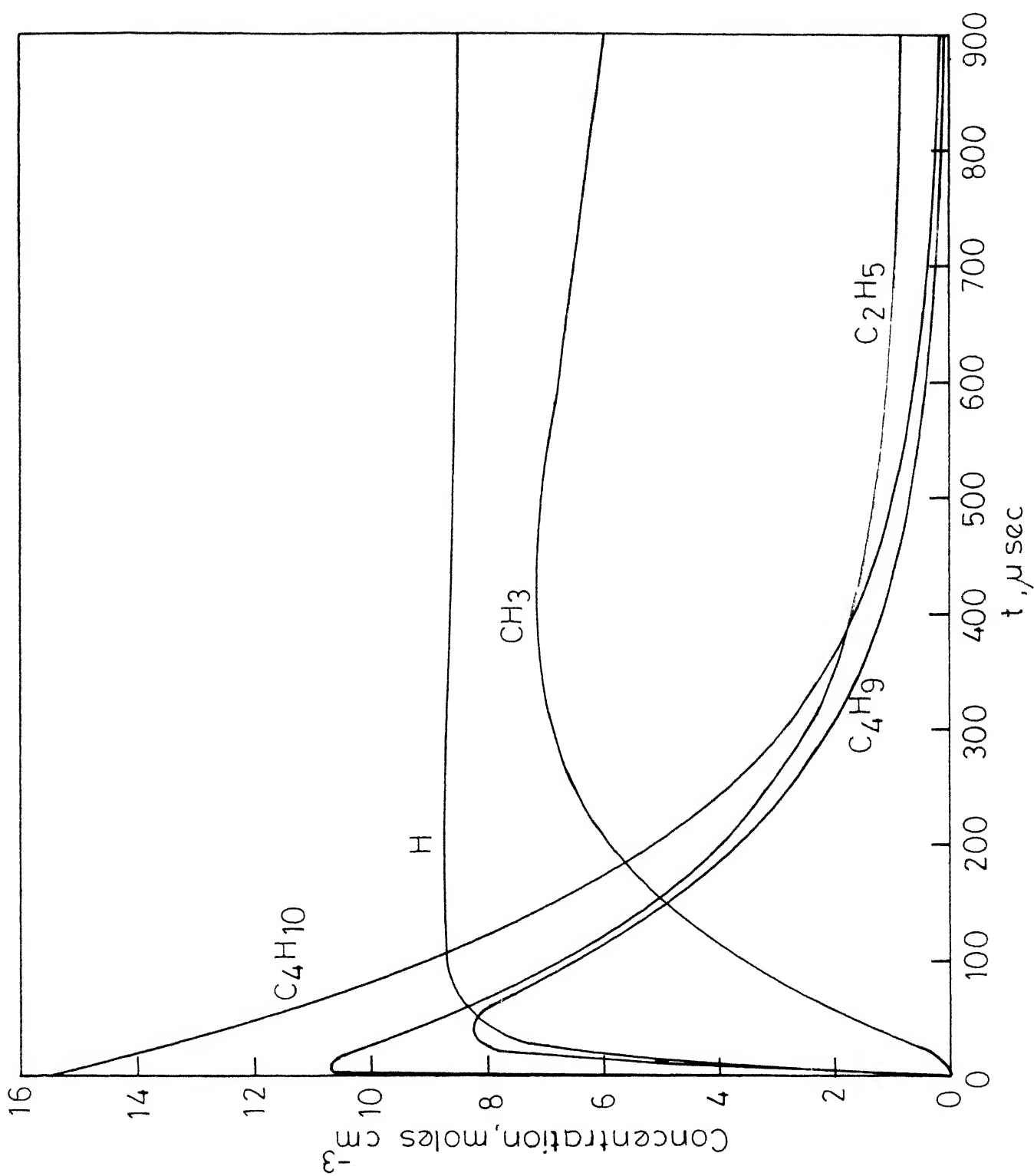


Fig. 5 - Concentration profiles for $T=1273^{\circ}\text{K}$, $p_2/p_1=12.9$ and $\text{C}_4\text{H}_{10}:\text{Ar}=9.8:90.2$.
 $10^7[\text{C}_4\text{H}_{10}], 10^{11}[\text{C}_4\text{H}_9], 10^{11}[\text{C}_2\text{H}_5]$
 $10^7[\text{CH}_3], 10^8[\text{H}]$
 $p_1=1\text{ torr}$

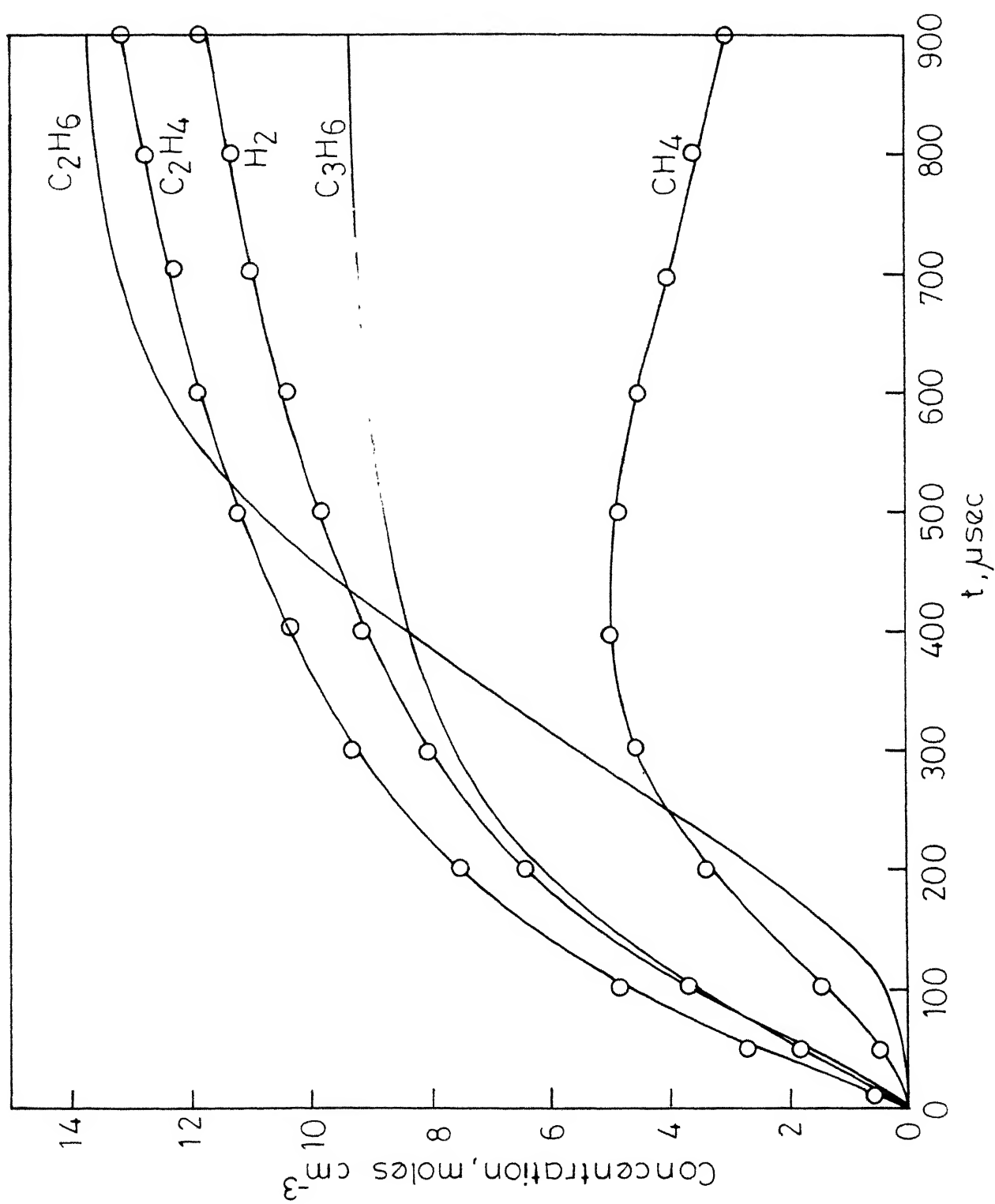


Fig. 6 - Concentration profiles for $T=1273^\circ\text{K}$, $p_2/p_1=12.9$ and $p_1=1\text{ torr}$
 $\text{C}_4\text{H}_{10}:\text{Ar}=9.8:90.2$
 $10^7[\text{C}_3\text{H}_6], 10^8[\text{C}_2\text{H}_6], [\text{C}_2\text{H}_4]10^6, 10^9[\text{CH}_4], 10^7[\text{H}]$

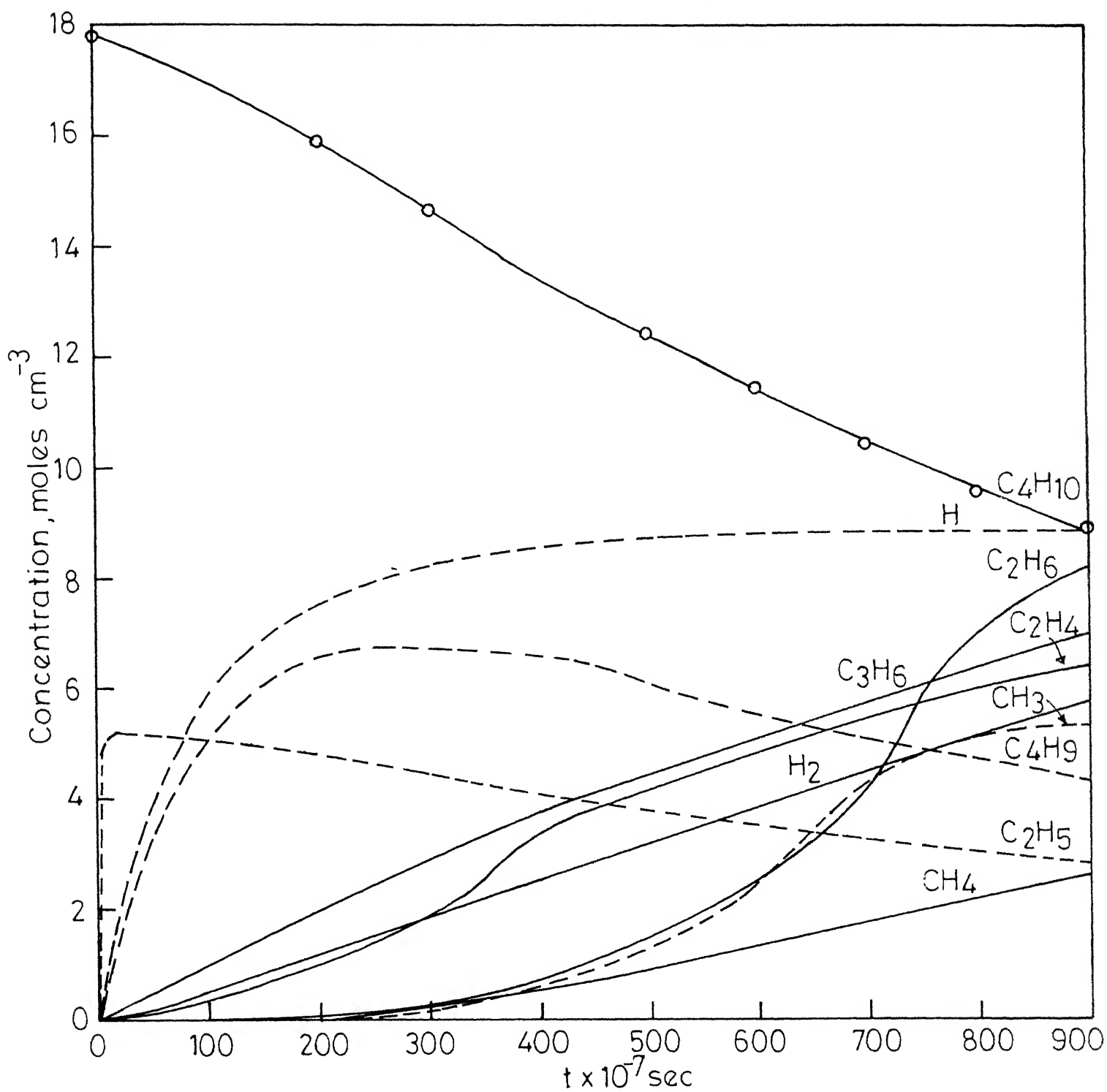


Fig. 7 - Concentration profile for $p_2/p_1=16.5$, $T=1391^\circ\text{K}$ and $p_1=1$ torr
 $\text{C}_4\text{H}_{10}:\text{Ar}=9.8:90.2$.

$10^6[\text{C}_4\text{H}_{10}]$, $10^{11}[\text{C}_4\text{H}_9]$, $10^7[\text{C}_3\text{H}_6]$, $10^7[\text{C}_2\text{H}_6]$, $10^{11}[\text{C}_6\text{H}_5]$
 $10^7[\text{C}_2\text{H}_4]$, $10^9[\text{CH}_4]$, $10^7[\text{CH}_3]$, $10^7[\text{H}]$, $10^8[\text{H}]$

APPENDIX 1

A LISTING OF THE PROGRAM TO COMPUTE THE EQUILIBRIUM VALUES OF
PRESSURE, TEMPERATURE AND DENSITY

ILIN=60

IZ=0

D = 129500.0

OPEN(UNIT=1, FILE='SHOCK.COR')

TYPE300

TYPE200

DO 502 I=1,25

READ(1,500)Y,U1,D21A

FORMAT(3F10.3)

FORMAT(2X,F15.5,2X,6(F14.8,2X)/)

FORMAT(2X,10X,'U1',12X,'T2',19X,'Z',12X,'CP21',12X,'P21',14X,'

1D21',13X,'Y'//)

FORMAT(1H0,10X,70H BUTANE+AR FROZEN SHOCK CALCULATION WITH BUTANE

1 CONCENTRATION = 0.09800//)

R=8.317E+07

R1=1.987

T1=298.15

W1=41.724

X=0.09800

CP1=5.2620

A11=+3.2768608E00

A21=+7.080814E-01

A31=-5.833118E-06

A41=-1.5832666E-08

A51=0.0

A61=0.0

B11=+2.9437494E00

B21=+8.348578E-02

B31=-3.4431026E-05

B41=+7.10413E-09

B51=0.0

B61=0.0

W11=58.0

A12=+3.1364326E00

A22=+1.3089609E-03

A32=+2.1837364E-06

A42=-3.9518236E-12

A52=0.0

A62=0.0

B12=+3.8116451E00

B22=+7.8066107E-04

B32=-3.2336127E-07

B42=+6.3513203E-11

B52=0.0

B62=0.0

W12=48.066

A13=+3.0212591E00

A23=-2.1737249E-03

A33=+3.7542204E-06

A43=-2.9047200E-09

A53=0.0

A63=0.0

B13=+2.5372567E00

B23=-1.8422190E-05

B33=-8.8017921E-09

B43=+5.9643621E-12

B53=0.0

B63=0.0

W13=16.00

A14=4.8675

A24=0.0

A34=0.0

A44=0.0

A54=0.0

A64=-1.4810601E03

B14=4.8765

B24=0.0

B34=0.0

B44=0.0

B54=0.0

B64=-1.4810601E03

W14=39.94

H1=((A11*T1+A21*T1**2/2.+A31*T1**3/3.+A41*T1**4/4.)*X+(A14*T1+A6

14/T1)*(1.-X))

X1=X*(1.-Y)/(1.+Y*X)

X2=Y*X/(1.+Y*X)

X3=Y*X/(1.+Y*X)

X4=(1.-X)/(1.+Y*X)

```

A1=A11*X1+A12*X2+A13*X3+A14*X4
A2=A21*X1+A22*X2+A23*X3+A24*X4
A3=A31*X1+A32*X2+A33*X3+A34*X4
A4=A41*X1+A42*X2+A43*X3+A44*X4
A5=A51*X1+A52*X2+A53*X3+A54*X4
A6=A61*X1+A62*X2+A63*X3+A64*X4
B1=B11*X1+B12*X2+B13*X3+B14*X4
B2=B21*X1+B22*X2+B23*X3+B24*X4
B3=B31*X1+B32*X2+B33*X3+B34*X4
B4=B41*X1+B42*X2+B43*X3+B44*X4
B5=B51*X1+B52*X2+B53*X3+B54*X4
B6=B61*X1+B62*X2+B63*X3+B64*X4
W2=W11*X1+W12*X2+W13*X3+W14*X4
D21=D21A
10 D12=1./D21
P21=1.+(W1*U1**2*(1.-D12)/(R*T1))
DH2A=(U1**2)*(1.-(D12**2))/8.36E+07
T21=P21*D12*W2/W1
T2=T21*T1
Z=T2**(-1./3.)
12 IF(T2-790.)12,12,13
H2T=A1+A2*T2/2.+A3*T2**2/3.+A4*T2**3/4.+A5*T2**4/5.+A6/T2
CPT2=A1+A2*T2+A3*T2**2+A4*T2**3+A5*T2**4
GO TO 14
13 H2T=B1+B2*T2/2.+B3*T2**2/3.+B4*T2**3/4.+B5*T2**4/5.+B6/T2
CPT2=B1+B2*T2/2.+B3*T2**2+B4*T2**3+B5*T2**4
14 H2=((H2T*T2-U1)/W2)+(Y*X*D/((1.+Y*X)*W2))
CP21=CPT2/CP1
EPS=0.0001*(DH2A
16 IF(ABS(H2-DH2A)-EPS)17,17,16
D21=D21+0.00001
GO TO 10
17 IZ=IZ+1
IF(IZ-IZ/(I.IV*JLIN)19,18,19
18 TYPE102
102 FORMAT(1H1,///)
19 TYPE100,U1,T2,Z,CP21,P21,D21,Y
502 CONTINUE
STOP
END

```

A PROGRAM TO SOLVE SIMULTANEOUS DIFFERENTIAL EQUATIONS

```

*****
*THIS program solves a system of N first order ordinary differe*
*ntial equations using the Hamming's predictor - corrector*
*method. The program reads a starting value for the independent*
*variable X, the integration step size H, the upper limit of*
*integration XMAX, and N initial conditions YR(1)...YR(N). Y & F*
*are matrices containing solution and derivative values and are*
*described in the text. TE(J) is the truncation error estimate*
*for the corrector equation. COUNT is the step counter. The*
*FUNCTION RUNGE is called to integrate across the first three*
*steps and yields the starting value needed for the Hamming's*
*method. There after the equations are integrated using alternat*
*ely the predictor and corrector portions of the FUNCTION*
*HAMING. The equation being solved as an example are,  $0.2Y/DX2 = -Y$ *
*,  $Y(0)=0.0$ ,  $dy(0)/dx=1.0$ . to solve another system of differential*
*equations, all symbols referring to F and FR must be replaced*
*by statements defining the derivatives for the new system.*
*The solutions are PRINTed at the initial X, and after every*
*INF integration steps there after.
*****

INTEGER COUNT,RUNGE,HAMING
REAL K1,K2,K3,K4,K5,K6,K7,K8,K9,K10,K11,K12,K13,K14,MIXMW
DIMENSION TE(20),YR(20),FR(20),Y(4,20),F(3,20),W(10),CPR(10),HRT
1(10),MW(10)
OPEN(UNIT=1,DEVICE='DSK',FILE='ASS.CDR')
READ(1,*)X,H,XMAX,INT,N,(YR(J),J=1,N),(MW(J),J=1,N)
TYPE 200, H,XMAX,INT,N,(J,J=1,N)
TYPE 201, X,(YR(J),J=1,N)
K1=5.013E9
K2=-.865E11
K3=.4197E10
K4=-.1573E9
K5=.4075E11
K6=.7461E11
K7=.1902E14
K8=1.6E13
K9=1.0E13
K10=1.0E11
K11=1./E+12
K12=1.842E13
K13=3.056E13
K14=3.715E13
r=82.06
rr=1.987

P=1/760.0
COUNT=0
DO 2 J=1,N
TE(J)=0.
Y(4,J)=YR(J)
IF(RUNGE(N,YR,FR,X,H).NE.1) GO TO 4
FR(1)=-K1*YR(1)-(K2*YR(1))*YR(5)-(K5*YR(1))*YR(8)-(K7*YR(1))*YR(
110)+K8*(YR(5))**2
FR(2)=(K2*YR(1))*YR(5)-(K3*YR(2))-K4*YR(2)+(K5*YR(1))*YR(8)+(K7*
1YR(1))*YR(10)
FR(3)=K3*YR(2)
FR(4)=(K2*YR(1))*YR(5)+K9*YR(10)*YR(5)+K10*YR(8)^
12+K8*YR(5)^2-K12*YR(4)*YR(10)
FR(5)=(2.*K1)*YR(1)-(K2*YR(1))*YR(5)+K4*YR(2)-K6*YR(5)-2.*(K8)*Y
1R(5)**2-K9*YR(10)*YR(5)-K11*YR(5)*YR(1)+K12*YR(4)*YR(10)-K14*YR
1(5)*YR(10)
FR(6)=K4*YR(2)+K6*YR(5)+K8*YR(5)^2+K11*YR(5)*YR(10)
FR(7)=(K5*YR(1))*YR(8)-K13*YR(7)*YR(10)
FR(8)=K3*YR(2)-(K5*YR(1))*YR(8)-K10*YR(8)^2+K13*YR(7)*YR(10)+2.
1*K14*YR(5)*YR(10)
FR(9)=(K7*YR(1))*YR(10)+K11*YR(5)*YR(10)+K12*YR(4)*YR(10)+K13*YR
1(10)*YR(7)
FR(10)=K6*YR(5)-(K7*YR(1))*YR(10)-K9*YR(10)*YR(5)-K11*YR(5)*YR(1

```

```

10)-K12*YR(4)*YR(10)-K13*YR(7)*YR(10)-K14*YR(10)*YR(5)
GO TO 3
COUNT = COUNT + 1
ISUB = 4-COUNT
DO 5 J=1,N
Y(ISUB,J)=YR(J)
F(ISUB,1)=-K1*YR(1)-(K2*YR(1))*YR(5)-(K5*YR(1))*YR(8)-(K7*YR(1))
1*YR(10)+K8*(YR(5)**2)
F(ISUB,2)=(K2*YR(1))*YR(5)-(K3*YR(2))-K4*YR(2)+(K5*YR(1))*YR(8)+
1(K7*YR(1))*YR(10)
F(ISUB,3)=K3*YR(2)
F(ISUB,4)=(K2*YR(1))*YR(5)+K9*YR(10)*YR(5)+K10*YR(
28)^2+K8*YR(5)^2-K12*YR(4)*YR(10)
F(ISUB,5)=(2.*K1)*YR(1)-(K2*YR(1))*YR(5)+K4*YR(2)-K6*YR(5)-2.*(K
18)*YR(5)^2-K9*YR(10)*YR(5)-K11*YR(5)*YR(10)+K12*YR(4)*YR(10)-K1
14*YR(10)*YR(5)
F(ISUB,6)=K4*YR(2)+K6*YR(5)+K8*YR(5)^2+K11*YR(5)*YR(10)
F(ISUB,7)=(K5*YR(1))*YR(8)-K13*YR(10)*YR(7)
F(ISUB,8)=K3*YR(2)-(K5*YR(1))*YR(8)-K10*YR(8)^2+K13*YR(10)*YR(7)
1+2.*K14*YR(5)*YR(10)
F(ISUB,9)=(K7*YR(1))*YR(10)+K11*YR(5)*YR(10)+K12*YR(4)*YR(10)+K1
13*YR(10)*YR(7)
F(ISUB,10)=K6*YR(5)-(K7*YR(1))*YR(10)-K9*YR(10)*YR(5)-K11*YR(5)
1*YR(10)-K12*YR(4)*YR(10)-K13*YR(7)*YR(10)-K14*YR(5)*YR(10)
IF(COUNT/INT*INT.EQ.COUNT) GO TO 7
IF(COUNT.LE.3) TYPE 202,X,(Y(ISUB,J),J=1,N)
IF(COUNT.GT.3) TYPE 202,X,(Y(1,J),J=1,N)
IF(X.GT.XMAX-H/2.) GO TO 1
IF(COUNT.GT.3) GO TO 3
M=H*INT(N,Y,F,X,H,TE)
F(1,1)=-K1*Y(1,1)-K2*Y(1,1)*Y(1,5)-K5*Y(1,1)*Y(1,8)-K7*Y(1,1)*Y(
11,10)+K8*(Y(1,5)**2)
F(1,2)=K2*Y(1,1)*Y(1,5)-K3*Y(1,2)-K4*Y(1,2)+K5*Y(1,1)*Y(1,8)+K7
1*Y(1,1)*Y(1,10)
F(1,3)=K3*Y(1,2)
F(1,4)=(K2*Y(1,1))*Y(1,5)+K9*Y(1,10)*Y(1,5)+K10*Y(
11,8)^2+K8*Y(1,5)^2-K12*Y(1,4)*Y(1,10)
F(1,5)=2.*K1*Y(1,1)-K2*Y(1,1)*Y(1,5)+K4*Y(1,2)-K6*Y(1,5)-2.*K8*Y
1(1,5)^2-K9*Y(1,10)*Y(1,5)-K11*Y(1,5)*Y(1,10)+K12*Y(1,4)*Y(1,10)
1-K14*Y(1,5)*Y(1,10)
F(1,6)=K4*Y(1,2)+K6*Y(1,5)+K8*Y(1,5)^2+K11*Y(1,5)*Y(1,10)
F(1,7)=(K5*Y(1,1))*Y(1,8)-K13*Y(1,7)*Y(1,10)
F(1,8)=K3*Y(1,2)-(K5*Y(1,1))*Y(1,8)-K10*Y(1,8)^2+K13*Y(1,7)*Y(1,
110)+2.*K14*Y(1,5)*Y(1,10)
F(1,9)=(K7*Y(1,1))*Y(1,10)+K11*Y(1,5)*Y(1,10)+K12*Y(1,4)*Y(1,10)
1+K13*Y(1,7)*Y(1,10)
F(1,10)=K6*Y(1,5)-(K7*Y(1,1))*Y(1,10)-K9*Y(1,10)*Y(1,5)-K11*Y(1,
15)*Y(1,10)-K12*Y(1,4)*Y(1,10)-K13*Y(1,7)*Y(1,10)-K14*Y(1,5)*Y(1
1,10)
SSUM1=0.0
DO 50 J=1,N
SSUM1=SSUM1+Y(1,J)
SSUM2=0.0
DO 60 J=1,N
SSUM2=SSUM2+(M*Y(1,J))
MIXMW=SSUM2/SSUM1
TYPE *,MIXMW
IF(M.EQ.1) GO TO 8
COUNT = COUNT + 1
GO TO 6
FORMAT(5X,F10.4,10X,F10.6,12X,F10.4/5X,15,15X,I2/
1(20X,4F12.5))
FORMAT(10H H =, E15.3/ 10H XMAX =, F12.4/ 10H INT
1=, 17/ 10H N =, 17/10H/ 10H 5X,10X, 4(2HY(,12,1H),10X
1)/ (1H,16X, 4(2HY(,12,1H),10X))
FORMAT(1H, E15.7, 4E15.7/ (1H, 10X, 4E15.7) )
FORMAT(1H, E15.7, 4E15.7/ (1H, 10X, 4E15.7))
END

```


FUNCTION HAMING(N,Y,F,X,H,TE)

```

*****
* HAMING IMPLEMENTS HAMING'S PREDICTOR-CORRECTOR ALGORITHM TO *
* SOLVE N SIMULTANEOUS FIRST ORDER DIFFERENTIAL EQUATIONS (ORDY) *
* X IS THE INDEPENDENT VARIABLE AND H IS THE INTEGRATION STEP *
* SIZE. THE ROUTINE MUST BE CALLED TWICE FOR INTEGRATION ACROSS *
* EACH STEP. IN THE FIRST CALL IT IS ASSUMED THAT THE SOLUTION *
* VALUES AND THE DERIVATIVE VALUES FOR THE N EQUATIONS ARE *
* STORED IN THE FIRST N COLUMNS OF THE FIRST FOUR ROWS OF THE *
* Y MATRIX AND FIRST THREE ROWS OF THE F MATRIX RESPECTIVELY. *
* THE ROUTINE COMPUTES N PREDICTED SOLUTIONS YPRED(J), INCREMENTS *
* X BY H AND PUSHES ALL VALUES IN Y&F MATRICES DOWN ONE ROW. *
* THE PREDICTED SOLNS YPRED(J) ARE MODIFIED, USING THE TRUNCATION *
* ERROR ESTIMATES TE(J) FROM THE PREVIOUS STEP, AND SAVED IN THE *
* FIRST ROW OF THE Y MATRIX. HAMING RETURNS TO THE CALLING PROGRAM *
* WITH THE VALUE 1 TO INDICATE THAT ALL DERIVATIVES SHOULD BE *
* COMPUTED AND STORED IN THE FIRST ROW OF THE F ARRAY BEFORE THE *
* SECOND CALL IS MADE ON HAMING. ON SECOND ENTRY TO THE FUNCTION *
* (DETERMINED BY LOGICAL VARIABLE PRED), HAMING USES THE HAMING *
* CORRECTOR TO COMPUTE NEW SOLUTION ESTIMATES, ESTIMATES THE *
* TRUNCATION ERRORS TE(J) FOR THE CURRENT STEP, IMPROVES THE *
* CORRECTED SOLUTIONS USING THE NEW TRUNCATION ERROR ESTIMATES *
* SAVES THE IMPROVED SOLUTIONS IN THE FIRST ROW OF THE Y MATRIX *
* AND RETURNS TO THE CALLING PROGRAM WITH A VALUE 2 TO INDICATE *
* COMPLETION OF ONE INTEGRATION STEP
*****

```

INTEGER HAMING

LOGICAL PRED

DIMENSION YPRED(20), TE(N), Y(4,N), F(3,N)

DATA PRED / .TRUE. /

IF(.NOT.PRED) GO TO 4

DO 1 J=1,N

YPRED(J) = Y(4,J) + 4.*H*(2.*F(1,J)-F(2,J)+2.*F(3,J))/3.

DO 2 J=1,N

DO 2 K5=1,3

K = 5 - K5

Y(K,J)=Y(K-1,J)

IF(K.LT.4) F(K,J)=F(K-1,J)

DO 3 J=1,N

Y(1,J)=YPRED(J)+112.*TE(J)/9.

X=X+H

PRED = .FALSE.

HAMING = 1

RETURN

DO 5 J=1,N

Y(1,J) = (9.*Y(2,J)-Y(4,J)+3.*H*(F(1,J)+2.*F(2,J)-F(3,J)))/8.

TE(J) = 9.*(Y(1,J)-YPRED(J))/121.

Y(1,J)=Y(1,J)+TE(J)

PRED = .TRUE.

HAMING = 2

RETURN

END

FUNCTION RUNGE(N,Y,F,X,H)

```

*****
* THE FUNCTION RUNGE EMPLOYS FOURTH ORDER RUNGE-KUTTA METHOD *
* WITH RUNGE'S COEFF'S TO INTEGRATE A SYSTEM OF N SIMULTANEOUS *
* FIRST ORDER ORDINARY DIFFERENTIAL EQUATIONS F(J)=DY(J)/DX *
* J=1,N, ACROSS A STEP OF LENGTH H IN THE INDEPENDENT VARIABLE H *
* IN THE INDEPENDENT VARIABLE X, SUBJECT TO INITIAL CONDITION Y(J *
* ), J=1,N. EACH F(J), THE DERIVATIVE OF Y(J), MUST BE COMPUTED FOUR *
* TIMES PER INTEGRATION STEP BY CALLING THE PROGRAM. THE FUNCTION *
* MUST BE CALLED FIVE TIMES PER STEP, SO THAT THE INDEPENDENT *
* VARIABLE-VALUE (X) AND THE SOLN VALUES (Y(1,1)..Y(1,N)) CAN BE *
* UPDATED USING RUNGE KUTTA ALGORITHM. M-PASS COUNTER: *
*****

```

INTEGER RUNGE

DIMENSION PHI(50), SAVEY(50), Y(N), F(N)

DATA M/0/

M=M+1

GO TO (1,2,3,4,5), M

RUNGE=1

RETURN

DO 22 J=1,N

```

SAVEY(J) = Y(J)
PHI(J)=F(J)
22 Y(J)=SAVEY(J)+0.5*H*F(J)
X=X+0.5*H
RUNGE = 1
RETURN
3 DO 33 J=1,N
PHI(J)=PHI(J)+2.0*F(J)
33 Y(J)=SAVEY(J)+0.5*H*F(J)
RUNGE=1
RETURN
4 DO 44 J=1,N
PHI(J)=PHI(J)+2.*F(J)
44 Y(J)=SAVEY(J) + H*F(J)
X=X+.5*H
RUNGE=1
RETURN
5 DO 55 J=1,N
55 Y(J) = SAVEY(J)+(PHI(J)+F(J))*H/6.
M=0
RUNGE=0
RETURN
END

```